This article has been accepted for publication in a future issue of this journal, but has not been fully edited. Content may change prior to final publication. Citation information: DOI 10.1109/JESTPE.2018.2870985, IEEE Journal of Emerging and Selected Topics in Power Electronics

Finite-State Model Predictive Control with Integral Action Applied to a Single-Phase Z-Source Inverter

Roberto O. Ramírez, José R. Espinoza, *Member IEEE*, Carlos R. Baier, *Member IEEE*, Marco Rivera, *Member, IEEE*, Felipe Villarroel, Johan Guzman, *Member IEEE*, and Pedro E. Melín, *Member IEEE*

***Abstract*—Finite-State Model Predictive Control (FSC-MPC) can be applied to a power converter if there is an accurate existing model of the converter. The best results will be achieved if and only if the parameters and variables that make up the system are properly estimated. If this is not the case, the predictions made using these strategies may be erroneous and cause problems, such as steady-state error with respect to the assigned desired references. This work presents a predictive control strategy with integral action that compensates for the differences between the estimated model and the inverter with the objective of achieving zero steady-state error without requiring external loops or state observers. The proposed strategy is tested on a single-phase Z-source inverter (SP-ZSI) so as to evaluate the error in both the ac and dc controlled variables with respect to their references to their cosigns. The experimental results confirm that the proposed strategy achieves zero error in steady state while maintaining the fast dynamic response of the classic predictive control.**

***Index terms*— Predictive Control, Z-Source Inverter, FCS-MPC, DeadBeat, Steady state error.**

I. Introduction

MODEL Predictive Control (MPC), despite having been under development for nearly forty years, is still considered an emerging strategy in many industrial applications [1]-[3]. In applications that use power converters, Finite-State Model Predictive Control (FCS-MPC) has received attention from researchers and developers for more than a decade [4]-[7]. This interest is due to the fact that defining the mathematical models to predict the behavior of the variables in a converter is not usually very complicated; furthermore, the existence of inexpensive, powerful digital signal processors (DSP) for the implementation of these strategies is an advantage that was not available 20 or 30 years ago [8]-[10].

Nowadays, in the specific field of static power converters, three-phase and single-phase inverters are fundamental in power integration applications for incorporating renewable energy to the distributed grid systems, micro-grids and/or isolated systems [11]-[17]. Diverse types of inverters have been controlled using FS-MPC's. This strategy has been proposed in voltage source inverters (VSI), current source inverters (CSI) and also in Z-source inverter and quasi Z-source inverter (ZSI/qZSI) impedance networks [18].

Z-source inverters (ZSI/qZSI) are among the least-known inverters because they were first proposed less than 20 years ago [19]-[23]. These inverters have the advantage that they can behave as boosters or dampers on the ac-side, unlike VSIs, which can only act as dampers, or CSIs, which work as boosters [26][27]. This characteristic of Z-source inverters is considered a great advantage because it does not require the use of dc/dc converters to extend its operating ranges, which is a common practice with VSI's and CSI's [28]-[31].

Despite being easy to understand and implement, FCS-MPC presents a series of challenges that have yet to be overcome, including steady-state error [32]. This steady-state error is most evident when there are considerable differences between the discrete model and the system or when the FCS-MPC has a low DSP sampling frequency [33][34]. Considering that, in general in FSC-MPC's, the maximum switching frequency is related to the implemented DSP sampling frequency, there is a contradictory problem: in order to minimize the system's steady-state error, one must increase the sampling frequency, which in turn increases the converter's switching losses. In recent years, various works related to inverters implemented with FCS-MPCs have focused on better understanding the cause of this steady-state error, with the aim of reducing or eliminating it [33]-[38]. Among the most note-worthy works are those that propose state observers [39][44]. Nevertheless, depending on the type of converter and model, the implementation of these observers can be a complicated task given the requirement to have the models associated with the

Manuscript received April 15, 2018, revised July 10, 2018; accepted September 6, 2018. This work was supported by the Chilean Government under Project CONICYT/FONDECYT 1160969, Project CONICYT/FONDECYT 1160690 and CONICYT /DOCTORADO NACIONAL/ 21160928

R. O. Ramirez, C. R. Baier and M. Rivera are with the Department of Electro-mechanics and Energy Conversion, Universidad de Talca, Curicó 747-C, Chile (e-mail: roramirez@utalca.cl; cbaier@utalca.cl; marcoriv@utalca.cl).

J. R. Espinoza and F. Villarroel are with the Department of Electrical Engineering, Universidad de Concepción, Concepción 160-C, Chile (e-mail: jose.espinoza@udec.cl; fvillarroel@udec.cl).

J. I. Guzman and P. E. Melín are with the Department of Electrical and Electronic Engineering, Universidad del Bío-Bío, Concepción 5-C, Chile (e-mail: joguzman@ubiobio.cl; pemelin@ubiobio.cl).

This article has been accepted for publication in a future issue of this journal, but has not been fully edited. Content may change prior to final publication. Citation information: DOI 10.1109/JESTPE.2018.2870985, IEEE Journal of Emerging and Selected Topics in Power Electronics

system being studied.

A single-phase Z-source inverter (SP-ZSI), fed by a known dc voltage source, must regulate both its dc capacitor voltages and its dc inductor currents and track the current reference in the ac load. All of these variables are controlled by the four available states of the H-bridge converter. This work proposes the use of an FSC-MPC strategy for the SP-ZSI that achieves control and eliminates steady-state error in both the dc-side voltage and the ac load current. To that end, an integral action will be implemented in the ac current loop and the dc voltage loop without the use of external loops. The proposed strategy reduces the steady-state error caused by poor parameter estimations and/or changes in the load conditions. Since it is not necessary to increase the switching frequency in order to reduce the steady-state error, it is possible to reduce the switching losses with respect to the reduced error by using a higher sampling frequency in the control strategy; demonstrating this, however, falls outside the scope of this paper. Compared with traditional control strategies, the resulting control strategy is simple and intuitive to implement, and it eliminates the need to design multiple cascaded loops to control the SP-ZSI [24].

This work is organized as follows. The next section presents an overview of predictive control operations, and will also study the prediction errors present in these controllers. Section III presents SP-ZSI as a converter of interest for applications in the classic FSC-MPC strategy. Section IV gives the equations necessary for the proposed method to be applied in the impedance source inverter. Section V presents the experimental results obtained in an SP-ZSI under classic FSC-MPC and the proposed strategy and compares both strategies. Finally, Section VI offers the conclusions of this paper.

II. Finite State Model Predictive Control

Predictive control utilizes a model of the system to calculate the value of the state variables in a given prediction horizon and then selects the optimal input to meet the control objectives set for a given number of sampling times [1][2]. In particular, in the case of power converters, there are a finite number of inputs that permit changes in the values of the control variables [3]. These correspond to the permitted state combinations {1,0} or {open, closed} that each of the converter's switches can take. Thus, the control challenge is a hybrid system in which the state variables are continuous, but the inputs are discrete [45].

Given a system that is represented by the equation,

$$\dot{\mathbf{x}}(t) = \mathbf{A}\mathbf{x}(t) + \mathbf{B}\mathbf{u}(t,s) \tag{1}$$

where **x**(t) is the state variable vector, **u**(t) is the input vector, and *s* is the selected state out of a total of *n* possible states. From (1), it is possible to obtain a predictive model by using the forward Euler approximation as,

$$\dot{\mathbf{x}}(t) \approx \frac{x(k+1) - x(k)}{T_s} \tag{2}$$

The discrete model used to estimate the value of the state variables at an arbitrary sampling time k+1 corresponds to,

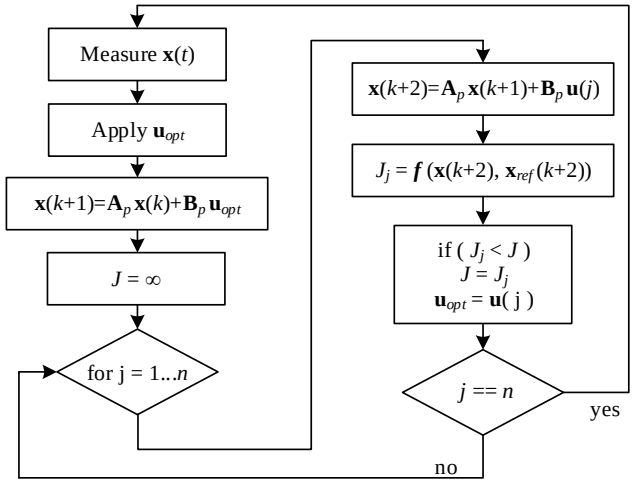

Fig. 1 Model Predictive Control strategy for power converters

$$\mathbf{x}(k+1) = \mathbf{A}_p\mathbf{x}(k) + \mathbf{B}_p\mathbf{u}(k) \tag{3}$$

where $\mathbf{A}_p$ and $\mathbf{B}_p$ are the state matrices associated with the discrete model defined as,

$$\mathbf{A}_p = \mathbf{I} + T_s\mathbf{A} \tag{4}$$

$$\mathbf{B}_p = T_s\mathbf{B} \tag{5}$$

Depending on the type of control scheme implemented, **u**(k) can be applied indirectly via a modulation stage or directly applied as a given switching state [4][27]. In this work, the latter is considered – Fig. 1 -. The input selection is carried out by evaluating a cost function *J*,

$$\mathbf{u}(k+1) = \min_{s=1,2,..n} J\left(\mathbf{u}(s), \mathbf{x}(k), \mathbf{x}_{ref}(k+1)\right) \tag{6}$$

Equation (1) is exact if and only if the sampling time tends to zero and the values of matrices $\mathbf{A}_p$ and $\mathbf{B}_p$ are known; in this case, the prediction will tend to have an error $\mathbf{e}_p(k+1)$ equal to zero. If these conditions are not met, there will be prediction errors that can lead to the selection of inputs that are not optimal and can cause steady-state error or slower or oscillatory dynamic responses [32]-[34].

Given that traditional predictive control does not log its prior inputs, or integral action, it is not possible to correct for this deviation once steady state is reached. Furthermore, it has been demonstrated that the control behaves as a high gain [46]; therefore, perfect reference tracking is not guaranteed in a zero order system. In order to avoid such problems, it is proposed that an integral action be incorporated into the predictive control with the aim of absorbing the differences between the model and the real system and thus obtain zero steady-state error. The next section will explore how to include said integral action into the proposed predictive model without requiring external loops.

This article has been accepted for publication in a future issue of this journal, but has not been fully edited. Content may change prior to final publication. Citation information: DOI 10.1109/JESTPE.2018.2870985, IEEE Journal of Emerging and Selected Topics in Power Electronics

III. Proposed Finite-State Model Predictive Control With Integral Action

Given the system's uncertainty,

$$\tilde{\mathbf{x}}(k+1) = \tilde{\mathbf{A}}_p \mathbf{x}(k) + \tilde{\mathbf{B}}_p \mathbf{u}^*(k) \tag{7}$$

where $\tilde{\mathbf{x}}$ is the error in the estimation of state variables, and $\tilde{\mathbf{A}}_p$ and $\tilde{\mathbf{B}}_p$ correspond to the state matrices with estimation error. The prediction error is defined as,

$$e_p(k+1) = x(k+1) - \tilde{x}(k+1) \tag{8}$$

or by replacing (3)-(7) in (8),

$$e_p(k+1) = \left(\mathbf{A}_p - \tilde{\mathbf{A}}_p\right)\mathbf{x}(k) + \mathbf{B}_p \mathbf{u}_{opt}(k) + \tilde{\mathbf{B}}_p \mathbf{u}^*(k) \tag{9}$$

with $\mathbf{u}^*(k)$ equal to the input chosen by the approximate system, which is not necessarily equal to that of the exact system $\mathbf{u}_{opt}$. At least, though, the prediction error is expected to be zero in the steady state with the aim of preventing steady-state error. By replacing this condition in (9), the input $\mathbf{u}^*(k)$ for which the system will have zero error in steady state is defined as,

$$\mathbf{u}^*(k) = -\tilde{\mathbf{B}}_p^{-1}\left(\mathbf{A}_p - \tilde{\mathbf{A}}_p\right)\mathbf{x}_{ref}(k) - \tilde{\mathbf{B}}_p^{-1}\mathbf{B}_p \mathbf{u}_{opt}(k), \tag{10}$$

which can be simplified to,

$$\mathbf{u}^*(k) = \mathbf{u}_{offset}(k) + \mathbf{K} \cdot \mathbf{u}_{opt}(k), \tag{11}$$

where,

$$\mathbf{u}_{offset}(k) = -\tilde{\mathbf{B}}_p^{-1}\left(\mathbf{A}_p - \tilde{\mathbf{A}}_p\right)\mathbf{x}_{ref}(k), \tag{12}$$

and

$$\mathbf{K} = -\tilde{\mathbf{B}}_p^{-1}\mathbf{B}_p. \tag{13}$$

Eq. (11) shows that the input necessary to compensate for the model changes can be broken down into the sum of the output of the two controllers, (i) one responsible for compensating for the model error $\mathbf{u}_{offset}$ and (ii) the other designed to track the imposed reference $\mathbf{u}_{opt}$. Therefore, to maintain a satisfying dynamic response - characteristic of the predictive control - and at the same time achieve zero as prediction error in steady state, it is necessary that the input $\mathbf{u}^*$ - applied on the model with uncertainty - be equal to an optimal input (obtained from the approximate model) plus an offset signal dependent on the difference between the matrices $\mathbf{A}_p$ and $\tilde{\mathbf{A}}_p$ of the exact and approximate models, respectively. This need for compensation becomes more evident by replacing (10) in (9), where the following expression is obtained:

$$e_p(k+1) = \left(\mathbf{A}_p - \tilde{\mathbf{A}}_p\right)\left(\mathbf{x}_{ref}(k) - \mathbf{x}(k)\right) \tag{14}$$

Clearly, (14) shows that the only condition that allows obtaining zero prediction error is given when the error between the reference and the controlled variable is null. Indeed, if the system model has uncertainty, the difference between $\mathbf{A}_p$ and $\tilde{\mathbf{A}}_p$ is constant and different from zero.

Thus, if $\mathbf{u}_{offset}$ is the input that makes the steady-state prediction error zero, and the variables $\mathbf{x}_{ref}$ and $\mathbf{x}$ are continuous, it can be shown from (12), that this input can also be expressed as:

$$\mathbf{u}_{offset}(z) = \frac{\mathbf{G}_i}{2}\frac{1+z^{-1}}{1-z^{-1}}\left(\mathbf{x}_{ref}(z) - \mathbf{x}(z)\right), \tag{15}$$

where $\mathbf{u}_{offset}$ will be the result of the discrete integral of the error between the reference and the controlled variable, where $\mathbf{G}_i$ is a gain that includes the term $\left(\mathbf{A}_p - \tilde{\mathbf{A}}_p\right)$.

Therefore, it is possible to propose a control strategy in which a $\mathbf{u}_{opt}$ signal is obtained from a standard predictive controller, and a $\mathbf{u}_{offset}$ signal generated by a pure integral controller, as seen in (15).

The output of is strategy is equivalent to the output of the PI controller in which $\mathbf{u}_{opt}$ corresponds to the proportional output

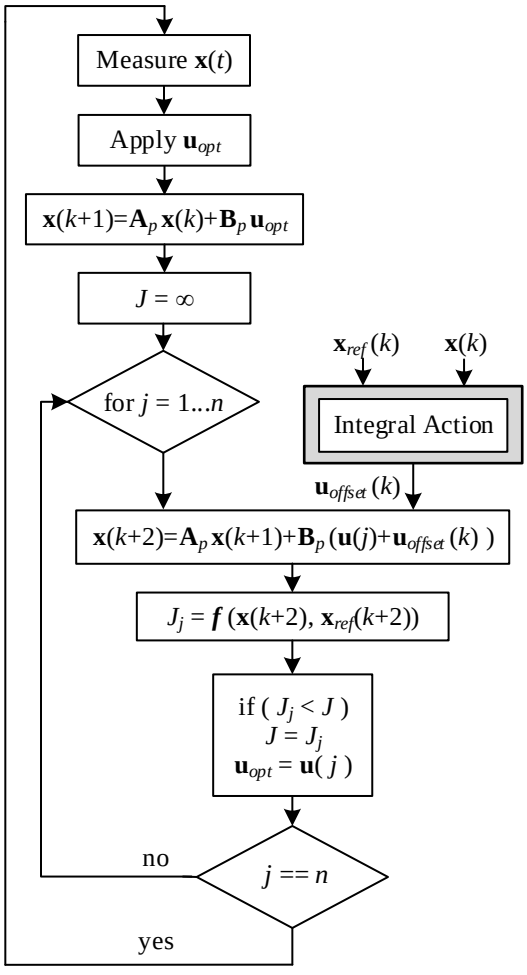

Fig. 2 Diagram of proposed predictive control.

This article has been accepted for publication in a future issue of this journal, but has not been fully edited. Content may change prior to final publication. Citation information: DOI 10.1109/JESTPE.2018.2870985, IEEE Journal of Emerging and Selected Topics in Power Electronics

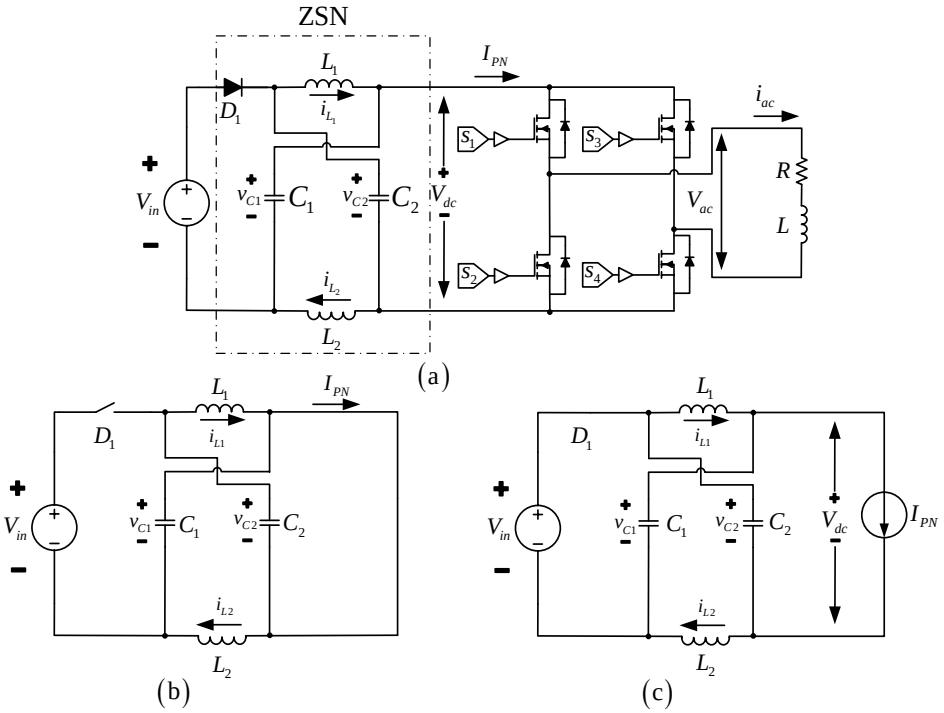

Fig. 3 Single-phase Z-source inverter. (a) Topology; (b) STS; (c) nSTS.

term and $\mathbf{u}_{offset}$ to the integral output control. A diagram of the proposed strategy can be seen in Fig. 2.

The optimal input $\mathbf{u}_{opt}$ derived from predictive control can be (*i*) continuous, as in the case of deadbeat predictive control [42][43], or (*ii*) discrete, as in the case of FS-MPC. In (*i*) the output is applied directly via a modulation stage, while in (*ii*) the new input $\mathbf{u}_{offset}$ must be included in a prediction equation as,

$$\tilde{x}(k+1) = \tilde{\mathbf{A}}_p \mathbf{x}(k) + \tilde{\mathbf{B}}_p \left(\mathbf{u}_{offset} + \mathbf{u}(s) \right) \qquad (16)$$

which is evaluated for each possible state *s* of the converter. It should be noted that there is no external control loop that calculates the input $\mathbf{u}_{offset}$ from a slower state variable; rather, both control actions take place simultaneously in the model, and they depend only on the error between the reference and the controlled state variable. Thus, there is no external dynamic that limits the proposed controller's response speed.

The next section explores the proposed integral predictive control strategy's performance. To that end, a single-phase Z-source inverter (SP-ZSI) is introduced as the inverter to be controlled since, from a control point of view, it presents challenges not found in voltage source or current source inverters.

IV. Model Predictive Control in SP-ZSI

A. Single-phase Z-source inverter

This inverter, which is fed by a dc source, consists of two main parts: the Z-source network (ZSN) and the H-bridge, as seen in Fig. 3(a). The ZSN corresponds to a non-linear network since, along with two condensers and two inductors, its topology requires a diode. This diode allows the ZSN and the H-bridge to endure a brief shoot-through state (STS), whose equivalent circuit can be seen in Fig. 3(b). When the inverter is not in STS, it is in non-shoot-through sate (see Fig. 3(c)), which is to considered to be two sub-states: the active sub-state, when power flows from the dc side to the ac side, and the inactive sub-state, when there is a zero that is not carried out by the STS.

B. Z-source inverter model

Considering the Z-source inverter's two states, it is possible to describe the model of the ZSN by first taking into account the STS state, in which the network diode is not considered to conduce. This leads to the following equations,

$$\frac{di_{L1}}{dt} = \frac{v_{C2}}{L_1} \qquad (17)$$

$$\frac{di_{L2}}{dt} = \frac{v_{C1}}{L_2} \qquad (18)$$

where i_{L1} and i_{L2} are the instantaneous currents and the inductances in the ZSN, respectively, while v_{C1} and v_{C2} are the instantaneous voltages and the capacitances in the network, respectively. L_1 and L_2 are the values of the inductances through which these currents circulate. Taking into account the dynamics of the ZSN capacitors leads to the following equations,

$$\frac{dv_{C1}}{dt} = -\frac{i_{L2}}{C_1} \qquad (19)$$

$$\frac{dv_{C2}}{dt} = -\frac{i_{L1}}{C_2} \qquad (20)$$

This article has been accepted for publication in a future issue of this journal, but has not been fully edited. Content may change prior to final publication. Citation information: DOI 10.1109/JESTPE.2018.2870985, IEEE Journal of Emerging and Selected Topics in Power Electronics

where C_1 and C_2 are the capacitances submitted to the voltages v_{C1} and v_{C2} in the ZSN. On the other hand, when the nSTS is considered, the voltage drop of the ZSN diode can be disregarded, and the current dynamics in the inductances can be expressed as,

$$\frac{di_{L1}}{dt} = \frac{1}{L_1}\left(V_{in} - v_{C1}\right) \tag{21}$$

$$\frac{di_{L2}}{dt} = \frac{1}{L_2}\left(V_{in} - v_{C2}\right) \tag{22}$$

where V_{in} is the inverter's dc supply voltage. Meanwhile, the capacitor voltages in the nSTS respond to the following dynamics,

$$\frac{dv_{C1}}{dt} = \frac{1}{C_1}\left(-I_{PN} + i_{L1}\right), \tag{23}$$

$$\frac{dv_{C2}}{dt} = \frac{1}{C_2}\left(-I_{PN} + i_{L2}\right), \tag{24}$$

where I_{PN} current is a variable that in the nSTS will depend on the values of the controlled current in the ac load and that in the STS it will depend on the controlled current and voltage (respectively) in the inductances and capacitances of the Z-source network in the dc side. Considering that the behavior of the currents and the voltages in the ZSN depends on whether it is operating in STS or nSTS, it is possible to define a condition variable for STS that represents the state of the network; this variable is expressed as follows,

$$S_{ST} = \begin{cases} 1 & if\ STS \\ 0 & if\ nSTS \end{cases} . \tag{25}$$

If the size of the Z-source network inductances L_1 and L_2 and the capacitances C_1 and C_2 are equal, then the following equation can be obtained from (17), (18), (20) and (21),

$$\frac{di_{Ln}}{dt} = \frac{1}{L_n}((2S_{ST} - 1)v_{Cn} + (1 - S_{ST})V_{in}) \tag{26}$$

Likewise, (19), (20), (23) y (24) lead to,

$$\frac{dv_{Cn}}{dt} = \frac{1}{C_n}(i_{Ln}(1 - 2S_{ST}) + I_{PN}(S_{ST} - 1)), \tag{27}$$

where i_{Ln} is the current in both inductances and v_{Cn} is the voltage in both of the Z-source network's capacitors.

From the discrete model, it is possible to define an average model and determine the general behavior as a function of an STS duty cycle, as follows,

$$\frac{di_{Ln}}{dt} = \frac{1}{L_n}((2d - 1)v_{Cn} + (1 - d)V_{in}) \tag{28}$$

and

$$\frac{dv_{Cn}}{dt} = \frac{1}{C_n}(i_{Ln}(1 - 2d) + I_{PN}(d - 1)) \tag{29}$$

In steady state, if the derivatives are considered as zero, it is found that the voltage gains from the duty cycle can be expressed as,

$$G_v = \frac{v_{Cn}}{V_{in}} = \frac{(1 - d)}{(1 - 2d)} \tag{30}$$

C. Classic FS-MPC in a single-phase Z-source inverter

One possible classic FS-MPC strategy in an SP-ZSI with a known RL load is that shown in Fig. 4*Fig.* . Here, based on the current and voltage prediction models in the components of the ZSN, a dc cost function is evaluated for the two possible inverter states, STS and nSTS. This cost function compares the voltage and current references with their respective predictions. Once evaluated, the state that minimizes the dc cost function is selected. In a similar process, the ac-side model predicts the behavior of the load current, which will depend on the voltage value V_{ac}. The voltage value can be $-V_{dc}$, zero or V_{dc}. The cost function evaluates the current prediction of each possible value concerning the reference; that which minimizes the cost function is selected.

Considering a Euler method discretization of the models given by (26) and (27) for the dc side of the inverter, it is possible to express the dc-side prediction equations as,

$$i_{Ln}(k+1) = \frac{T_s}{L_n}((2S_{ST} - 1)v_{Cn}(k) + (1 - S_{ST})V_{in}) + i_{Ln}(k) \tag{31}$$

and

$$v_{Cn(k+1)} = \frac{T_s}{C_n}((1 - 2S_{ST})i_{Ln}(k) + (S_{ST} - 1)I_{PN}(k)) + v_{Cn}(k), \tag{32}$$

where $i_{Ln}(k+1)$ are the future inductance currents in the ZSN that depend on a number of factors: the present measurement of the current $i_{Ln}(k)$ in any of the inductances, the present measurement of the voltage in any of the capacitances $v_{Cn}(k)$, the value of the supply voltage V_{in} and the STS condition variable (S_{ST}). On the other hand, $v_{Cn(k+1)}$ corresponds to the future voltage in any of the ZSN capacitors. The prediction equation (32) also depends on the H-bridge current input $I_{PN}(k)$, which can be estimated based on the measurement of the load current. Furthermore, because the inductance current should be minimized, the following reference current can be utilized during STS and nSTS,

$$i_{L_{ref}}(k) = (1 - S_{ST})h_{SW}(k)i_{ac_{ref}}(k), \tag{33}$$

This article has been accepted for publication in a future issue of this journal, but has not been fully edited. Content may change prior to final publication. Citation information: DOI 10.1109/JESTPE.2018.2870985, IEEE Journal of Emerging and Selected Topics in Power Electronics

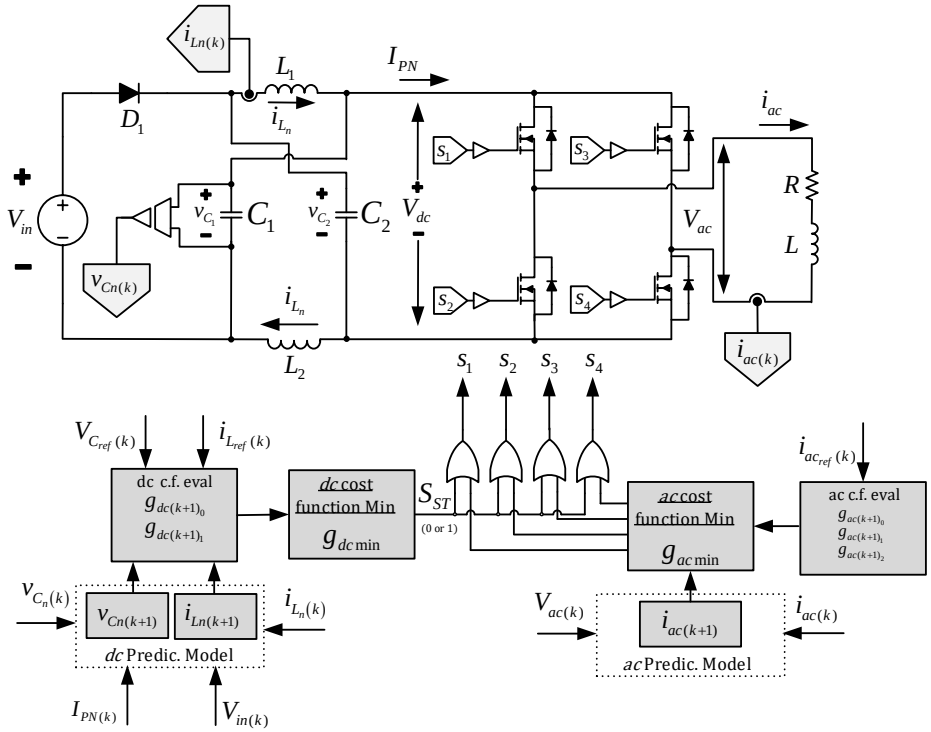

Fig. 4 Classic FCS-MPC in a SP-ZSI.

where $h_{SW}(k)$ can have the values{1,0,-1} and corresponds to the present switching state of the single-phase H-bridge in the nSTS, and $i_{ac_{ref}}$ is the ac-side current reference of the inverter (load reference).

Considering the reference given in (33), the dc-side cost function can be expressed as,

$$g_{dc(k+1)} = \lambda_i \left| i_{L_{ref}}(k) - i_{L_n}(k+1) \right| + \lambda_v \left| v_{C_{ref}(k)} - v_{C_n}(k+1) \right|, \quad (34)$$

where λ_i and λ_v are the weighting factors that allow the voltage control in the capacitors to be faster or slower with respect to the dc inductance currents. Properly selecting the weighting factors will slow the changes in the capacitors' voltages to limit the ZSN inductance currents better.

Finally, to implement the ac current control block, the current prediction model (i_{ac}) in the RL load and the cost function (g_{ac}) are expressed, respectively, by the following equations,

$$i_{ac}(k+1) = \frac{T_s}{L}\left(V_{ac(k)} - R i_{ac(k)}\right) + i_{ac}(k) \quad (35)$$

and

$$g_{ac}(k+1) = \left| i_{ac_{ref}}(k) - i_{ac}(k+1) \right| \quad (36)$$

with the prediction of the ac- and dc-side variables and the minimization of both cost functions, it is possible to determine the switching state that will optimize the reference tracking or come closest to the desired values. Nevertheless, it is well known that this tracking is optimal when the model parameters are correctly estimated, the weighting factors properly selected and there is an increased sampling frequency. The higher the sampling frequency, the more the basic FSC-MPC will be able to reduce steady-state error. At the same time, however, an increased sampling frequency will also increase the inverter's losses since the maximum switching frequency will be higher.

D.Proposal to eliminate steady-state error in the SP-ZSI.

As demonstrated in section III, it is possible to obtain zero steady-state error between the imposed reference and the controlled variable by making the prediction error null. In order to achieve this, it is necessary to define a new input to the predictive model, named $\mathbf{u}_{offset}$, that can compensate for the difference between the exact and the used model, using a pure integrator acting on the model and not on the reference as it happens when external loops are used. Thus, based on (16), a predictive control strategy with integral action has been designed to control the dc voltage in the capacitances and, at the same time, the ac load current in the SP-ZSI output, Fig. 5. The strategy seeks to eliminate steady-state error caused by a low switching frequency, errors caused by incorrect estimation of the parameters and model variables. The integral controller $\mathbf{u}_{offset}$ in each control loop - described in the previous section - is redefined as u_{dc} for the dc voltage control loop and u_{ac} for the ac current control loop when is applied to the SP-ZSI. Since the voltage in the capacitor to be controlled is dc, a pure integrator

This article has been accepted for publication in a future issue of this journal, but has not been fully edited. Content may change prior to final publication. Citation information: DOI 10.1109/JESTPE.2018.2870985, IEEE Journal of Emerging and Selected Topics in Power Electronics

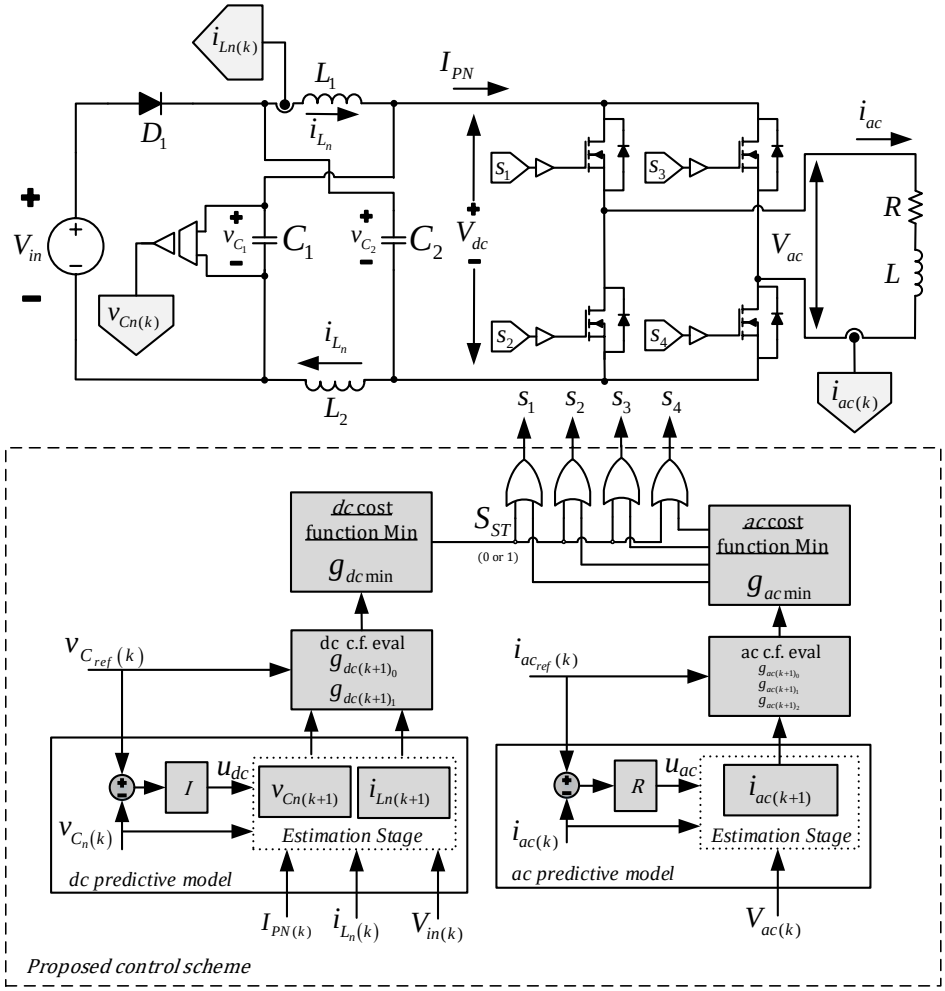

Fig.5. FSC-MPC proposed to eliminate steady-state error.

I can be used to generate the control u_{dc}; this integrator, implemented in the discrete Z domain, can be expressed as

$$u_{dc}(z) = \frac{T_s K_I}{2} \frac{1+z^{-1}}{1-z^{-1}} e_{dc}(z), \tag{37}$$

where T_s is the sampling period, K_I is an integral gain, and $e_{dc}(z)$ is the discrete dc reference error with respect to the measured dc variable. On the other hand, since a sinusoidal reference is imposed, a pure resonance R fulfills the integral action at frequency ω_o on the ac current loop; this resonance can be expressed in the Z domain using the impulse invariance method for its discrete implementation as,

$$u_{ac}(z) = K_r T_s \frac{1-z^{-1}\cos(\omega_0 T_s)}{1-2z^{-1}\cos(\omega_0 T_s)+z^{-2}} e_{ac}(z) \ , \tag{38}$$

where K_r is the resonance gain, ω_o is the fundamental frequency on the ac side, and e_{ac} (z) is the discrete reference error concerning the ac measurement. If both (37) and (38) are expressed discretely, then the following equation describes the dc control that will be programmed in the DSP,

$$\mathrm{u}_{dc}(k) = \frac{K_I T_s}{2}\left(e_{dc}(k) - e_{dc}(k-1)\right) + u_{dc}(k-1). \tag{39}$$

Likewise,

$$\mathrm{u}_{ac}(k) = K_r T_s e_{ac}(k) - e_{ac}(k-1) K_r T_s \cos(\omega_o T_s) + 2u_{ac}(k-1)\cos(\omega_o T_s) - u_{ac}(k-2) \ , \tag{40}$$

corresponds to the ac control that will be programmed in the DSP. Thus, the new prediction equations (31) - (32) are defined as,

$$i_{ac}(k+1) = \frac{T_s}{L}(V_{ac}(k) - R i_{ac}(k) + \mathrm{u}_{ac}(k)) + i_{ac}(k) \tag{41}$$

and

This article has been accepted for publication in a future issue of this journal, but has not been fully edited. Content may change prior to final publication. Citation information: DOI 10.1109/JESTPE.2018.2870985, IEEE Journal of Emerging and Selected Topics in Power Electronics

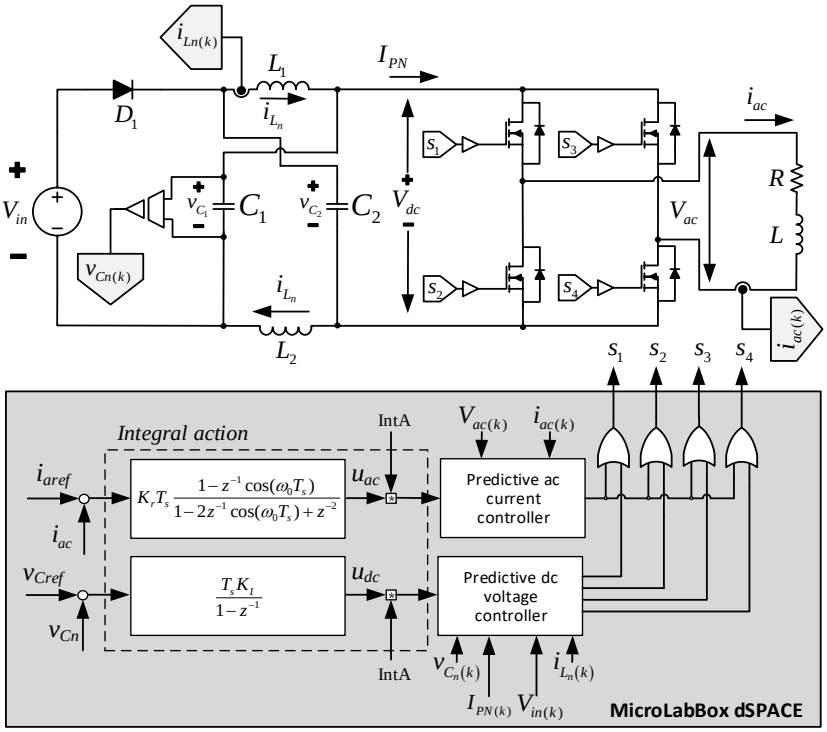

Fig. 6 Diagram of experimental set-up implemented in the laboratory.

$$v_{Cn(k+1)} = \frac{T_s}{C_n}((1-2S_{ST})i_{Ln}(k) + (S_{ST}-1)I_{PN}(k) + \mathrm{u}_{dc}(k)) + v_{Cn}(k) \quad (42)$$

where $u_{ac}(k)$ and $u_{dc}(k)$ are the resonant control outputs and the discrete integral, respectively. Meanwhile, the proposed cost functions are exactly the same as (34) for the dc side and (36) for the ac side.

The gain of each $\mathbf{u}_{offset}$ terms can be designed to ensure that the dynamics of the predictive controller and the integral controllers do not overlap (interfere). This way, the time constants should be at least 5~10 times slower than the implemented sampling times. In each case, only one gain needs to be manipulated, so fulfilling this task is simple compared to the traditional linear methods in which cascade loops are used to control the dc-side voltage and current [24][25].

V. Experimental Results

In this section, the MPC schemes (standard and proposed) have been implemented controlling both the dc voltage in the capacitors and the ac current of an SP-ZSI that is feeding a slightly inductive load, to demonstrate that the proposed strategy works correctly. The sampling frequency is just 10kHz, to make the existence of a steady-state error even more evident. This low sampling frequency will produce a THD that could be smaller by merely operating at a higher sampling frequency. Fig. 6 shows the diagram of the implementation. Here, it can be seen that a dSPACE MicrolabBox has been used to simultaneously implement a classic FSC-MPC strategy an FSC-MPC strategy with the proposed integral action in such a way that it is possible to alternate between the classic FSC-MPC and the proposed strategy. An IntA signal enables alternation between the two strategies from a dSPACE control console. The parameters of the experimental set-up are given in Table 1 along with some of the key implementation values.

One issue that is important to highlight is that both predictive strategies have been tested with a sampling frequency of 20kHz. This frequency is relatively low in an SP-ZSI, which prevents the variables that are to be controlled by an FSC-MPC in both dc and ac from reaching the desired values.

TABLE 1

SET-UP PARAMETERS

Variables	Description	Values
V_{in}	Source Voltage	30[V]
L_1 & L_2	Z Network Inductors	1.5[mH]
C_1 & C_2	Z Network Capacitors	470[uF]
R_L	Resistance Load	17[Ω]
L_L	Inductor Load	25[mH]
f_0	Output frequency	50[Hz]
f_S	Sample frequency	20[kHz]
v_{ref1}	dc voltage steady state reference	65[V]
i_{acref}	ac load current steady state reference	2[A]
λ_i	Weighting Factor ZSN for Inductor Current	0.15
λ_v	Weighting Factor ZSN for Capacitor Voltage	1.2
K_I	Integral Gain for dc voltage control	2.5
K_r	Resonant gain for ac current control	1.5

This article has been accepted for publication in a future issue of this journal, but has not been fully edited. Content may change prior to final publication. Citation information: DOI 10.1109/JESTPE.2018.2870985, IEEE Journal of Emerging and Selected Topics in Power Electronics

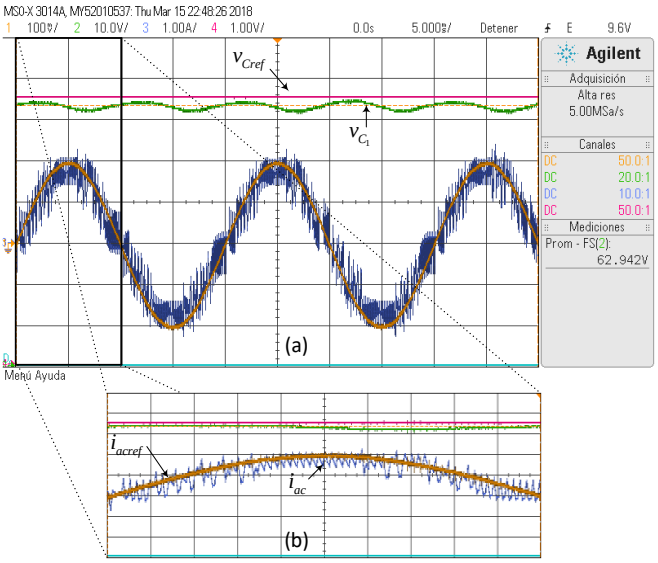

Fig. 7 Steady-state response of classic predictive control.

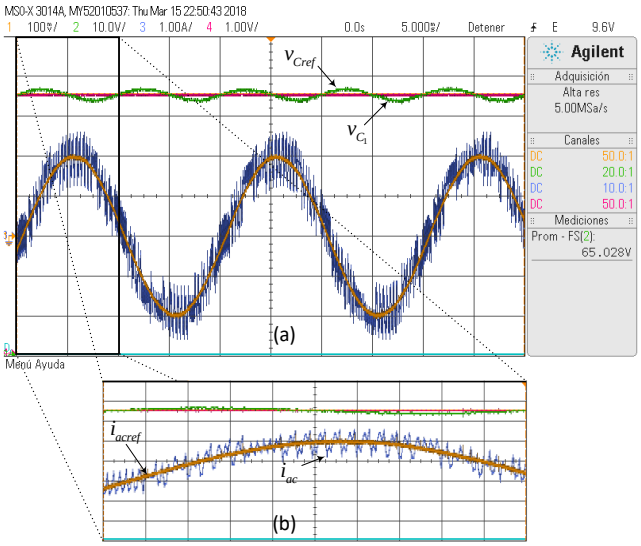

Fig. 8 Steady-state response of proposed integral predictive control.

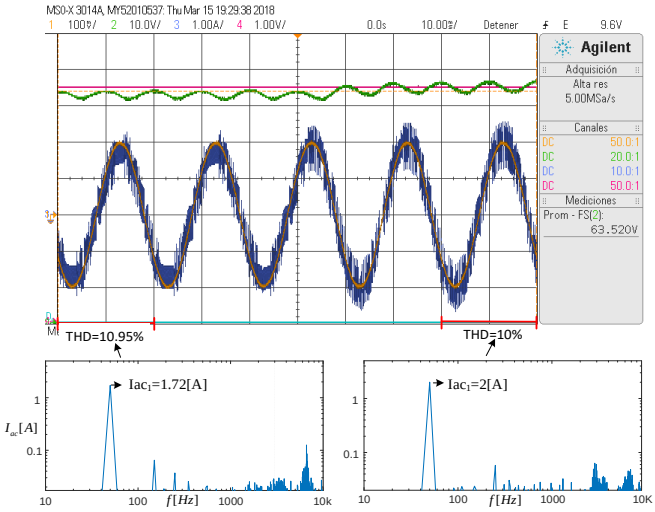

Fig. 9 Dynamic response. Transition from classic predictive control to proposed integral predictive control.

Furthermore, given the RL load parameters in Table 1 and the sampling frequency, there is a total harmonic distortion (THD) in the ac load current that is close to 20%.

The first experiment carried out on the prototype was under the classic FSC-MPC; it was provided with references and sought to maintain 65[V] in each capacitor and an amplitude of 2[A] in the alternate load current. As can be seen in Fig. 7(a) y Fig. 7(b), the classic FSC-MPC strategy does not achieve the proposed objectives since the average dc voltage is around 62.94[V] while the average current amplitude calculated in the load was 1.72[A]. Therefore, the steady-state error is 3.16[%] on the dc side with an average amplitude error of 14[%] on the ac side. The problem depicted in Fig. 7 implies an error in the desired power of the system since, if a power control system were to provide this inverter with these dc voltage references and ac current references, it would not be able to achieve the desired values.

The waveforms seen in Fig. 8(a) and Fig. 8(b) demonstrate that when the FSC-MPC with the integral action proposed in this work is first tested in steady state in the experimental set-up, it achieves very precise reference tracking and accomplishes zero steady-state error in both the dc voltage in the ZSN condensers and the ac load current in a highly practical way. Thus, it is demonstrated that the proposed strategy functions properly in steady state and achieves its objectives.

In order to evaluate the system's dynamic performance when the integral mode is activated, an experiment is performed in which the system starts out with the classic FSC-MPC strategy (IntA=0 in the diagram in Fig. 6) and then changes to the integral mode (IntA=1) partway through the acquisition. Fig. 9

This article has been accepted for publication in a future issue of this journal, but has not been fully edited. Content may change prior to final publication. Citation information: DOI 10.1109/JESTPE.2018.2870985, IEEE Journal of Emerging and Selected Topics in Power Electronics

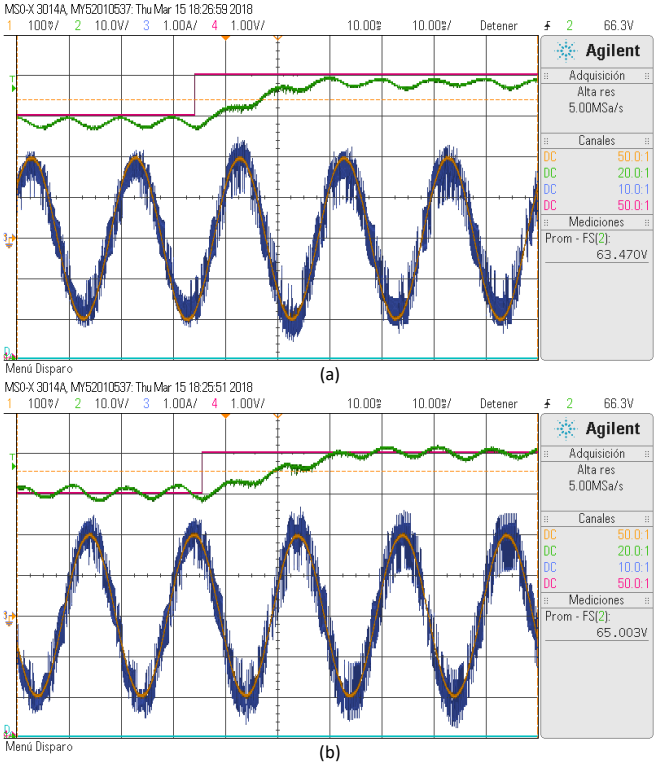

Fig. 10 Dynamic response to a change in the dc voltage reference. (a) Classic predictive control; (b) Proposed integral predictive control.

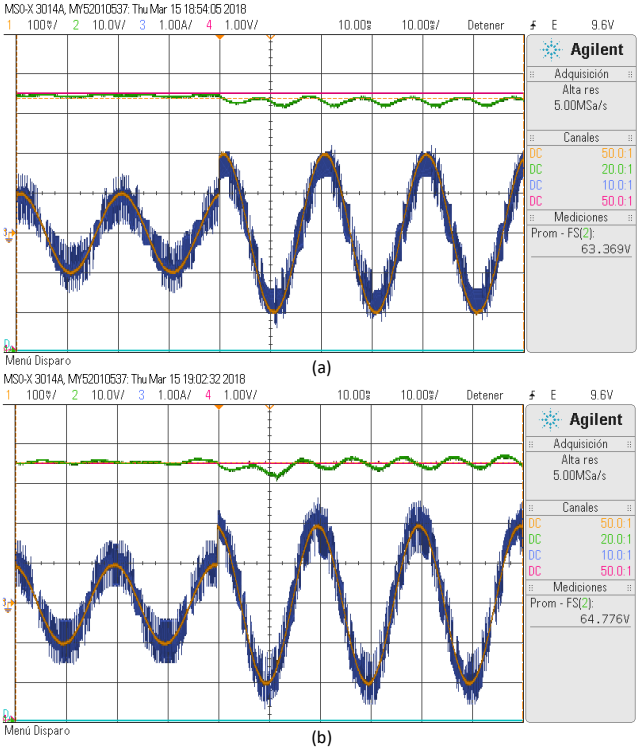

Fig. 11 Dynamic response to a change in the ac load. (a) Classic predictive control; (b) Proposed integral predictive control.

shows the voltage and current waveforms along with their references. Here, it can be seen that the system initially presents steady-state error for both the dc voltage, whose reference is 65[V] and the ac load current, whose amplitude reference is 2[A]. The integral control is activated partway through the acquisition (see Fig. 9(a)), and it can be clearly seen that in the dc control loop, the voltage takes around one cycle to reach the given reference, eliminating steady-state error. Meanwhile, on the ac side, the integral action (resonant) takes much less than a cycle to reduce steady-state error in the load current. If the harmonic content of the current in the RL load is obtained (Fig.9(b) classic control and Fig.9(c) proposed control), it is possible to see that in both cases the frequency values remain below 10kHz and that despite the fact that a comparison between Fig. 9(b) Fig. 9(c) would seem to indicate an increase in the harmonic content when the steady-state error is eliminated; the harmonic distortion decreases slightly in the correction from 10.95% to 10%, which is due to the significant increase in the fundamental value of nearly 14%.

In order to demonstrate that the integral controllers' actions (u_{ac} and u_{dc}) achieve the objectives without affecting the FSC-MPC strategy's dynamic behavior, a test is performed with a reference change for the dc voltage in the SP-ZSI condensers. This change is from 60[V] to 70[V] and takes place during the second acquisition cycle (see Fig. 10(a)). Here, the system's response without integral action (IntA=0) is observed, where the dynamic response takes about one cycle; nevertheless, since there is no integral action, the controlled variables (capacitors' dc voltages and the load current) do no achieve their assigned references.

Fig. 10(b) shows that in an oscilloscope the same signals as those in Fig. 10(a) are obtained, but with an added integral action in the system (that is, doing IntA=1). In this figure, it can be seen that the system starts with zero steady-state error in both the dc voltage and the ac current and that when confronted with a sudden change in the dc voltage reference, the dynamic response is that of a critically damped system. It is important to remember that this response adjustment is carried out primarily with the gain K_I of the integral controller u_{dc}. Finally, Fig. 10(b) shows that the ac current maintains a tracking with zero steady-state error at all times. The THD of the load currents have been calculated in steady state for each of the conditions observed in Fig. 10(a) and Fig. 10(b), concluding that there is minor distortion when the steady-state error is corrected, which is principally due to the significant increase in the fundamental frequency.

Finally, an impact on the load is made in the system via a change in the ac current reference for both the classic predictive implementation and the proposed strategy with integral action. Fig. 11(a) shows the response of the classic predictive system without integral action under a load change from 50% to 100%. It can be seen that there is steady-state error independent of the load condition, though it is greater when the current demand increases due to the load. On the other hand, in the response of

the system using integral action on the dc and ac sides, shown in Fig. 11(b), it can be seen that the load impact occurs during the second current cycle (from 50 to 100%) achieving correct reference tracking in both ac and dc with zero error in steady state. At the time of the current load increase, it is observed that the dc voltage is slightly affected, reducing the dc value, which recovers an average of 65V in less than a cycle. This last waveform demonstrates that the proposed strategy behaves as intended, eliminating steady-state error in both the dc and ac sides without negatively impacting the dynamic performance of the classic predictive strategy.

VI. Conclusion

This work proposes a predictive control with an integral action aimed at eliminating the steady-state error innate to predictive strategies when confronted with parameter variations, load condition changes, and low switching frequencies, among others. The proposed strategy was obtained based on a mathematical analysis of the prediction error in the model; this was used to define the input required to compensate for the deviation of the control variable and its desired reference. Based on this analysis, it was determined that the necessary input is made up of two terms, one associated with the predictive controller, and the other with the model error. The latter can be compensated by employing just one integral action, as proposed in this work. The analysis shows that the structure obtained is similar to that of a PI controller in an exact linear system, but here the predictive controller carries out the proportional action. The resulting strategy relies on only one loop, and it does not require slower external loops to compensate for reference deviations. Furthermore, the use of an integrator or pure resonance provides a degree of independence for loop tuning, thus making this design simpler than those of linear cascade strategies.

With the objective of testing the proposed strategy for both the dc and ac variables, its application in an SP-ZSI converter was proposed. The experimental results showed a suitable performance in both steady and dynamic states. When compared to a classic predictive strategy, it is found that the proposed strategy is able to compensate for steady-state error in both ac and dc variables without impacting the dynamic response. In the experimental tests of the system without the proposed integral action, it is observed that the dc voltage error depends on the converter's ac load condition. This problem does not occur when the proposed strategy is implemented; it achieves zero error in the reference tracking for the load conditions evaluated. Thus, the proposed strategy is a considerable improvement over the classic algorithm used in these topologies as it maintains the transient dynamic characteristics while improving the steady-state performance.

References

[1] P. D. Roberts, "A brief overview of model predictive control", in *Proc. IEEE Sem. Practical Exp. Predictive Control*, Feb. 16, 2000, pp. 1-3.

[2] J. H. Lee, "Model predictive control: Review of the three decades of development", *Int. J. Control Automat. Syst.*, vol. 9, no. 3, pp. 415-424, Jun. 2011

[3] P. Cortes, M. P. Kazmierkowski, R. M. Kennel, D. E. Quevedo and J. Rodriguez, "Predictive Control in Power Electronics and Drives", in *IEEE Transactions on Industrial Electronics*, vol. 55, no. 12, pp. 4312-4324, Dec. 2008.

[4] S. Kouro, P. Cortes, R. Vargas, U. Ammann, and J. Rodriguez, "Model predictive control-a simple and powerful method to control power converters", *IEEE Trans. Ind. Electron.*, vol. 56, no. 6, pp. 1826–1838, Jun. 2009.

[5] M. Rivera, P. Wheeler, J. Rodriguez and B. Wu, "A review of predictive control techniques for matrix converter applications", *IECON 2017 - 43rd Annual Conference of the IEEE Industrial Electronics Society*, Beijing, 2017, pp. 7360-7365.

[6] R. H. Kumar, A. Iqbal and N. C. Lenin, "Review of recent advancements of direct torque control in induction motor drives – a decade of progress", in *IET Power Electronics*, vol. 11, no. 1, pp. 1-15, Jan. 2018.

[7] F. Wang, X. Mei, J. Rodriguez and R. Kennel, "Model predictive control for electrical drive systems-an overview", in *CES Transactions on Electrical Machines and Systems*, vol. 1, no. 3, pp. 219-230, Sep. 2017.

[8] S. Lucia, D. Navarro, Ó. Lucía, P. Zometa and R. Findeisen, "Optimized FPGA Implementation of Model Predictive Control for Embedded Systems Using High-Level Synthesis Tool", in *IEEE Transactions on Industrial Informatics*, vol. 14, no. 1, pp. 137-145, Jan. 2018.

[9] J. L. Jerez, P. J. Goulart, S. Richter, G. A. Constantinides, E. C. Kerrigan and M. Morari, "Embedded Online Optimization for Model Predictive Control at Megahertz Rates", in *IEEE Transactions on Automatic Control*, vol. 59, no. 12, pp. 3238-3251, Dec. 2014.

[10] V. Yaramasu and B. Wu, "Predictive Control of a Three-Level Boost Converter and an NPC Inverter for High-Power PMSG-Based Medium Voltage Wind Energy Conversion Systems", in *IEEE Transactions on Power Electronics*, vol. 29, no. 10, pp. 5308-5322, Oct. 2014.

[11] T. Dragičević, "Model Predictive Control of Power Converters for Robust and Fast Operation of AC Microgrids", in *IEEE Transactions on Power Electronics*, vol. 33, no. 7, pp. 6304-6317, July 2018.

[12] Z. Liu, C. Xiang, Y. Wang, Y. Liao and G. Zhang, "A Model-Based Predictive Direct Power Control for Traction Line-Side Converter in High-Speed Railway", in *IEEE Transactions on Industry Applications*, vol. 53, no. 5, pp. 4934-4943, Sept.-Oct. 2017.

[13] R. P. Aguilera *et al*., "Selective Harmonic Elimination Model Predictive Control for Multilevel Power Converters", in *IEEE Transactions on Power Electronics*, vol. 32, no. 3, pp. 2416-2426, March 2017.

[14] T. Dragičević, X. Lu, J. C. Vasquez and J. M. Guerrero, "DC Microgrids—Part I: A Review of Control Strategies and Stabilization Techniques", in *IEEE Transactions on Power Electronics*, vol. 31, no. 7, pp. 4876-4891, July 2016.

[15] F. Blaabjerg, M. Liserre and K. Ma, "Power Electronics Converters for Wind Turbine Systems", in *IEEE Transactions on Industry Applications*, vol. 48, no. 2, pp. 708-719, March-April 2012.

[16] S. M. Malik, X. Ai, Y. Sun, C. Zhengqi and Z. Shupeng, "Voltage and frequency control strategies of hybrid AC/DC microgrid: a review", in *IET Generation, Transmission & Distribution*, vol. 11, no. 2, pp. 303-313, Jan. 2017.

[17] W. Xiao, M. S. El Moursi, O. Khan and D. Infield, "Review of grid-tied converter topologies used in photovoltaic systems", in *IET Renewable Power Generation*, vol. 10, no. 10, pp. 1543-1551, Nov. 2016.

[18] B. Singh, B. N. Singh, A. Chandra, K. Al-Haddad, A. Pandey and D. P. Kothari, "A review of three-phase improved power quality AC-DC converters", in *IEEE Transactions on Industrial Electronics*, vol. 51, no. 3, pp. 641-660, June 2004.

[19] Fang Zheng Peng, "Z-source inverter", in *IEEE Transactions on Industry Applications*, vol. 39, no. 2, pp. 504-510, Mar.-Apr. 2003.

[20] W. Qian, F. Z. Peng and H. Cha, "Trans-Z-Source Inverters", in *IEEE Transactions on Power Electronics*, vol. 26, no. 12, pp. 3453-3463, Dec. 2011.

[21] M. K. Nguyen, Y. C. Lim and G. B. Cho, "Switched-Inductor Quasi-Z-Source Inverter", in *IEEE Transactions on Power Electronics*, vol. 26, no. 11, pp. 3183-3191, Nov. 2011.

[22] Y. P. Siwakoti, F. Z. Peng, F. Blaabjerg, P. C. Loh and G. E. Town, "Impedance-Source Networks for Electric Power Conversion Part I: A

Topological Review", in *IEEE Transactions on Power Electronics*, vol. 30, no. 2, pp. 699-716, Feb. 2015.

[23] Y. P. Siwakoti, F. Z. Peng, F. Blaabjerg, P. C. Loh, G. E. Town and S. Yang, "Impedance-Source Networks for Electric Power Conversion Part II: Review of Control and Modulation Techniques", in *IEEE Transactions on Power Electronics*, vol. 30, no. 4, pp. 1887-1906, April 2015.

[24] Y. Liu, H. Abu-Rub, and B. Ge, "Z-source/quasi-Z-source inverters: Derived networks, modulations, controls, and emerging applications to photovoltaic conversion", *IEEE Ind. Electron. Magazine*, vol. 8, no. 4, pp. 32-44, Dec. 2014

[25] K. W. Lee and T. Kim, "Operating-point insensitive voltage control of the Z-source inverter based on an indirect capacitor current control" in *IET Power Electronics*, vol. 8, no. 8, pp. 1358-1366, Aug. 2015.

[26] B. Wu, J. Pontt, J. Rodriguez, S. Bernet and S. Kouro, "Current-Source Converter and Cycloconverter Topologies for Industrial Medium-Voltage Drives", in *IEEE Transactions on Industrial Electronics*, vol. 55, no. 7, pp. 2786-2797, July 2008.

[27] M. P. Kazmierkowski and L. Malesani, "Current control techniques for three-phase voltage-source PWM converters: a survey", in *IEEE Transactions on Industrial Electronics*, vol. 45, no. 5, pp. 691-703, Oct 1998.

[28] C. D. Townsend, Y. Yu, G. Konstantinou and V. G. Agelidis, "Cascaded H-Bridge Multilevel PV Topology for Alleviation of Per-Phase Power Imbalances and Reduction of Second Harmonic Voltage Ripple" in *IEEE Transactions on Power Electronics*, vol. 31, no. 8, pp. 5574-5586, Aug. 2016.

[29] W. Li and X. He, "Review of Nonisolated High-Step-Up DC/DC Converters in Photovoltaic Grid-Connected Applications", in *IEEE Transactions on Industrial Electronics*, vol. 58, no. 4, pp. 1239-1250, April 2011.

[30] Q. Li and P. Wolfs, "A Review of the Single Phase Photovoltaic Module Integrated Converter Topologies With Three Different DC Link Configurations", in *IEEE Transactions on Power Electronics*, vol. 23, no. 3, pp. 1320-1333, May 2008.

[31] J. M. Carrasco et al., "Power-Electronic Systems for the Grid Integration of Renewable Energy Sources: A Survey", in *IEEE Transactions on Industrial Electronics*, vol. 53, no. 4, pp. 1002-1016, June 2006.

[32] H. A. Young, M. A. Perez and J. Rodriguez, "Analysis of Finite-Control-Set Model Predictive Current Control With Model Parameter Mismatch in a Three-Phase Inverter", in *IEEE Transactions on Industrial Electronics*, vol. 63, no. 5, pp. 3100-3107, May 2016.

[33] R. P. Aguilera, P. Lezana and D. E. Quevedo, "Switched Model Predictive Control for Improved Transient and Steady-State Performance", in *IEEE Transactions on Industrial Informatics*, vol. 11, no. 4, pp. 968-977, Aug. 2015.

[34] K. H. Ahmed, A. M. Massoud, S. J. Finney and B. W. Williams, "A Modified Stationary Reference Frame-Based Predictive Current Control With Zero Steady-State Error for LCL Coupled Inverter-Based Distributed Generation Systems", in *IEEE Transactions on Industrial Electronics*, vol. 58, no. 4, pp. 1359-1370, April 2011.

[35] H. T. Nguyen and J. W. Jung, "Disturbance-Rejection-Based Model Predictive Control: Flexible-Mode Design With a Modulator for Three-Phase Inverters", in *IEEE Transactions on Industrial Electronics*, vol. 65, no. 4, pp. 2893-2903, April 2018.

[36] T. Dragičević, "Model Predictive Control of Power Converters for Robust and Fast Operation of AC Microgrids" in *IEEE Transactions on Power Electronics*, vol. 33, no. 7, pp. 6304-6317, July 2018.

[37] H. Lin and Z. Wang, "Virtual-multilevel model predictive control with error feedback for modular multilevel converters", in *IET Generation, Transmission & Distribution*, vol. 12, no. 3, pp. 531-539, Feb. 2018.

[38] C. Qi, X. Chen, P. Tu and P. Wang, "Deadbeat control for a single-phase cascaded H-bridge rectifier with voltage balancing modulation", in *IET Power Electronics*, vol. 11, no. 3, pp. 610-617, Mar. 2018.

[39] Z. Yin, X. Han, C. Du, J. Liu and Y. Zhong, "Research on Model Predictive Current Control for Induction Machine Based on Immune-optimized Disturbance Observer", in *IEEE Journal of Emerging and Selected Topics in Power Electronics*, vol. PP, no. 99, pp. 1-1.

[40] J. Wang, F. Wang, G. Wang, S. Li and L. Yu, "Generalized Proportional Integral Observer-Based Robust Finite Control Set Predictive Current Control for Induction Motor Systems with Time-Varying Disturbances", in *IEEE Transactions on Industrial Informatics*, vol. PP, no. 99, pp. 1-1.

[41] H. Yang, Y. Zhang, J. Liang, J. Liu, N. Zhang and P. Walker, "Robust Deadbeat Predictive Power Control with a Discrete-time Disturbance Observer for PWM Rectifiers under Unbalanced Grid Conditions" in *IEEE Transactions on Power Electronics*, vol. PP, no. 99, pp. 1-1.

[42] B. Wang, Z. Dong, Y. Yu, G. Wang and D. Xu, "Static-Errorless Deadbeat Predictive Current Control Using Second-Order Sliding-Mode Disturbance Observer for Induction Machine Drives" in *IEEE Transactions on Power Electronics*, vol. 33, no. 3, pp. 2395-2403, March 2018.

[43] X. Zhang, B. Hou and Y. Mei, "Deadbeat Predictive Current Control of Permanent-Magnet Synchronous Motors with Stator Current and Disturbance Observer" in *IEEE Transactions on Power Electronics*, vol. 32, no. 5, pp. 3818-3834, May 2017.

[44] G. Pannocchia and A. Bemporad, "Combined Design of Disturbance Model and Observer for Offset-Free Model Predictive Control", in *IEEE Transactions on Automatic Control*, vol. 52, no. 6, pp. 1048-1053, June 2007.

[45] A. Bemporad, W. P. M. H. Heemels and B. De Schutter, "On hybrid systems and closed-loop MPC systems", in *IEEE Transactions on Automatic Control*, vol. 47, no. 5, pp. 863-869, May 2002.

[46] R. O. Ramírez, J. R. Espinoza, F. Villarroel, E. Maurelia and M. E. Reyes, "A Novel Hybrid Finite Control Set Model Predictive Control Scheme With Reduced Switching," in *IEEE Transactions on Industrial Electronics*, vol. 61, no. 11, pp. 5912-5920, Nov. 2014.

Roberto O. Ramírez was born in Concepción, Chile, in 1988. He received the B.Sc. and Engineer degrees in electronic engineering (with first class honors), and the M.Sc. degree in electrical engineering from the University of Concepción, Concepción, Chile, in 2009, 2011, and 2013, respectively. Currently, he is Professor in the Faculty of Engineering, Universidad de Talca, Talca, Chile.

His research interest includes predictive control strategies, power converters, Robotics and embedded system development.

Jose R. Espinoza (S' 92–M' 97) received the Engineer degree in electronic engineering and the M.Sc. degree in electrical engineering from the University of Concepción, Concepción, Chile, in 1989 and 1992, respectively, and the Ph.D. degree in electrical engineering from Concordia University, Montreal, QC, Canada, in 1997. Since 2006, he has been a Professor with the Department of Electrical Engineering, University of Concepción, where he is engaged in teaching and research in the areas of automatic control and power electronics. He has authored/coauthored more than 200 refereed journal and conference papers and is an Associate Editor of the IEEE TRANSACTIONS ON INDUSTRIAL INFORMATICS.

Carlos R. Baier (S'08–M'11) was born in Temuco, Chile, in 1979. He received the B.S., M.Sc., and D.sc. degrees in electrical engineering from the University of Concepcion, Concepcion, Chile, in 2004, 2006, and 2010, respectively. Since 2009, he has been a Professor in the Faculty of Engineering, Universidad de Talca, Talca, Chile, where he is teaching in the areas of industrial electronics. His research interests include improved control techniques for multicell converters, emerging converters and strategies to inject power into the grid and high energy efficient improvements for medium-voltage converters.

This article has been accepted for publication in a future issue of this journal, but has not been fully edited. Content may change prior to final publication. Citation information: DOI 10.1109/JESTPE.2018.2870985, IEEE Journal of Emerging and Selected Topics in Power Electronics

Marco Rivera (S'09-M'11-SM'2017) received his B.Sc. in Electronics Engineering and M.Sc. in Electrical Engineering from the Universidad de Concepcion, Chile, in 2007 and 2008, respectively. He received his PhD degree from the Department of Electronics Engineering, Universidad Tecnica Federico Santa Maria, in Valparaiso, Chile, in 2011 with a scholarship from the Chilean Research Fund CONICYT. During 2011 and 2012, Prof. Rivera held a Post Doctoral position and worked as part-time professor of Digital Signal Processors and Industrial Electronics at Universidad Tecnica Federico Santa Maria. Currently he is an Associate Professor in the Faculty of Engineering at Universidad de Talca, Curicó, Chile. Prof. Rivera Abarca was awarded a scholarship from the Marie Curie Host Fellowships for early stage research training in electrical energy conversion and conditioning technology at the University College Cork, Cork, Ireland in 2008. In 2012, Prof. Rivera was awarded the Chilean Academy of Science Doctoral Thesis Award (Premio Tesis de Doctorado Academia Chilena de Ciencias), for the best PhD thesis published in 2011, selected from among all national and international students enrolled in any exact or natural sciences program in Chile and also he was awarded as an Outstanding Engineer in 2015. His research interests include matrix converters, predictive and digital controls for high-power drives, four-leg converters, renewable energies and development of high performance control platforms based on Field-Programmable Gate Arrays.

Felipe Villarroel received the B.Sc. and Engineer degree in electronic engineering (with first-class honors), and the M.Sc. degree in electrical engineering from the University of Concepción, Concepción, Chile, in 2007, 2009, and 2012, respectively. He is currently pursuing the Ph.D. degree in electrical engineering at the same institution, sponsored by a scholarship from the Chilean Research Foundation CONICYT starting from 2016. Since late 2012 until Feb. 2016, Mr. Villarroel worked as a hardware/software engineer at CADETECH S.A., Concepción, Chile. His research interests include the modeling, simulation and control of power converters, in particular predictive control techniques.

Johan I. Guzman (S'04–M'09) was born in Chile in 1976. He received his Electronic Engineering Title, his M.Sc. and D.Sc. degrees in electrical engineering from the University of Concepcion in 2000, 2007 and 2009 respectively. Since 2006 to 2008 he was lecturer at the University of Concepcion and the University of Desarrollo. Currently he is at the University of Talca where he has been since 2008, holding the position of assistant professor since 2010. He has consulting experience on energetic efficiency and integration of new technologies for little and medium business. His active research topics are power converters control for magnetic coupled converters and use of ERNC in isolated communities.

Pedro E. Melín C. (S'10, M'14) was born in Chillán, Chile, in 1982. He received the Eng. degree in Electronic Engineering, the M.Sc., degree and the D.Sc. degree in Electrical Engineering from the University of Concepción, Concepción, in 2006, 2010 and 2014 respectively. Since 2013, he has been with the Department of Electrical and Electronic Engineering, University of Bío-Bío, Concepción, Chile, where he is assistant professor teaching in the areas of electronic applications and digital systems. His research interest include voltage-source and current-source converters and their extension to multilevel topologies, including their design, digital control and the application of this kind of topologies to AC drives, active power filters and energy conversion.